Iraqi Journal of Market Research and Consumer Protection
(2024) 16(1): 38-57
DOI: http://dx.doi.org/10.28936/jmracpc16.1.2024.(4)
Abdulsada et al.

المجلة العراقية لبحوث السوق
وحماية المستهلك

PREPARATION OF NEW COMPLEXES OF METHYL METHACRYLAT WITH POLYVINYL ALCOHOL AND STUDY OF SOME ENVIRONMENTAL APPLICATIONS

Zainab S. Abdulsada[1*], Sanaa H. Awad[2] Sahar S. Hassan[3]
[1]Ministry of Environment, Baghdad, Iraq. zainab.sabeer1105a@csw.uobaghdad.edu.iq.
[2]Assist. Prof. Department of Chemistry, College of Science for woman, University of Baghdad, Iraq.sanaha_chem@csw.uobaghdad.edu.iq,
[3]Assist. prof. Department of Chemistry, College of Science for woman, University of Baghdad, Iraq.sahar_chem@csw.uobaghdad.edu.iq,

Received 8/ 3/ 2023, Accepted 3/ 7/ 2023, Published 30/ 6/ 2024

ABSTRACT

A new copolymer from Methyl methacrylate and polyvinyl alcohol [methyl-5-hydroxy-2-methylhexanoate] and its complexes were synthesized for some metals (Cr^{+3}, Mn^{+2}, Fe^{+3}, Co^{+2}, Ni^{+2}, Cu^{+2}, Zn^{+2}, Cd^{+2}). This ligand and its metal complexes were characterized using (FTIR) spectral, UV-Vis spectroscopy, conductivity, magnetic moment, and Thermo Gravimetric analysis. The nanoparticles for two complexes were characterized using x-ray diffraction, scanning electron microscope, and atomic force microscope. Zeolite 5A was prepared from local kaolin by hydrothermal preparation, then characterization, and used as a supporting material with prepared copolymer as a composite to remove several metals from polluted water taken from industrial water electric power stations in Dora and South of Baghdad. Trace concentrations of these metals were estimated before and after applying the prepared copolymer by atomic absorption spectroscopy. The removal using composite materials is significantly more effective, with the concentration recorded as very low and the concentrations of some metal ions like Fe^{+2}, which completely disappeared from polluted water according to a polluted water analysis before and after using the produced compounds.

Keywords: Removal of metal contaminants, Copolymer, Methyl methacrylate, Metal complexes, and Zeolite.

تحضير معقدات جديدة لمثيل ميثا اكريلت مع بولي فنيل الكحول ودراسة بعض التطبيقات البيئية .

زينب صبير عبد السادة [1] سناء هتور عواد[2] سحر صبيح حسن[3]
[1]وزارة البيئة، بغداد، العراق، zainab.sabeer1105a@csw.uobaghdad.edu.iq.
[2] الاستاذ المساعد الدكتور، قسم الكيمياء، كلية العلوم للبنات، جامعة بغداد، بغداد، العراق، sanaha_chem@csw.uobaghdad.edu.iq,
[3] الاستاذ المساعد الدكتور، قسم الكيمياء، كلية العلوم للبنات، جامعة بغداد، بغداد، العراق، sahar_chem@csw.uobaghdad.edu.iq,

الخلاصة:

في هذا العمل حضرنا بوليمر مشترك جديد من ميثيل ميثا أكريلات مع بولي فنيل الكحول [ميثيل-5-هيدروكسي-2-ميثيل هكسانوات] مع بعض العناصر الثقيلة (Cr^{+3}، Mn^{+2}، Fe^{+3}، Co^{+2}، Ni^{+2}، Cu^{+2}، Zn^{+2}، Cd^{+2}) لإنتاج المعقدات المقابلة. تم تشخيص ميثيل-5- هيدروكسي-2-ميثيل هكسانوات المحضر ومعقداته باستخدام طيف الأشعة تحت الحمراء والتحليل الطيفي المرئي للأشعة فوق البنفسجية، والتوصيلية والعزم المغناطيسي، وانحراف الأشعة السينية، ومجهر المسح الإلكتروني ومجهر القوة الذرية. تم استخدام البوليمر المشترك المحضر لإزالة عدد من العناصر من المياه الملوثة المسحوبة من المياه الصناعية لمحطات توليد الطاقة الكهربائية في الدورة وجنوب بغداد وتقدير التراكيز الضئيلة لهذه العناصر قبل وبعد استخدام البوليمر المشترك المحضر باستخدام مطيافية الامتصاص الذري. تعتبر الإزالة باستخدام المواد المتراكبة أكثر فاعلية بشكل ملحوظ مع تسجيل التركيز على أنه

[*]**The research is extracted from the doctoral thesis of the first researcher.**

منخفض جدًا واختفت تمامًا تراكيز بعض أيونات المعادن مثل Fe^{+2} من المياه الملوثة وفقًا لتحليل المياه الملوثة قبل وبعد استخدام المركبات المحضرة.

الكلمات المفتاحية: إزالة ملوثات المعادن ، بوليمر مشترك ، مثيل ميثا اكريلايت، معقدات المعادن والزيولايت.

INTRODUCTION

Water contamination continues to pose a threat to people's health on a global scale **(Soubh *el al.*, 2018)**. Metal poisoning offers a severe risk because of its toxicity, non-biodegradability, and bioaccumulation in the food chain **(Ashvinder, *el al.*, 2021)**. Industrial waste is the leading cause of heavy metal contamination in water systems. The effective removal of hazardous ions from wastewater is an important and urgent issue due to its negative and direct effects on flora and fauna. As a result of heavy metals ingested by other species in the food chain, their carcinogenic effects on humans and animals were increased. These metals are absorbed by plants, which then pass them to animals and humans **(Mahmoud *el al.*, 2020)**.

A hydrophilic polymeric network forms the three-dimensional structures known as hydrogels. They are cross-linked polymer networks containing water in them. Hydrophilic functional groups connected to the polymeric backbone absorb water, whereas cross-links between network chains allow them to resist dissolution **(Balbir *el al.*, 2021)**. Alcohols, carboxylic acids, amides, and other hydrophilic groups are among the hydrophilic groups that give hydrogels their hydrophilicity **(Tain *el al.*, 2021)**. Polymer gels play an essential role in many technical fields like gene delivery and drug delivery **(Noreen *el al.*, 2022)**, scaffolds for tissue engineering **(Abdullah *el al.*, 2021)** and superabsorbent materials because of their exceptional characteristics, such as biocompatibility and smart response behavior **(Pishnamazi *el al.*,2021)**. In the past, polymers made from methyl methacrylate have been used to remove dyes in environmentally friendly ways **(Uzma *el al.*, 2022)**.

Zeolites are available in two types: natural zeolites, which are non-porous and synthetic zeolites, which are porous and have a structure. They are prepared by heating soda ash, feldspar, and china clay together. Compared to natural zeolites, these have a higher exchange capacity per unit weight. **(Karmen & Anamarija, 2022)**.

Zeolites can potentially remove various chemicals, such as heavy metals, organic compounds, dyes, pigments, reagents, and nitrogen compounds, due to their cationic exchange negative charge features and relatively low production cost **(Luciano *el al.*, 2022)**, They are used as efficient adsorbents for various environmental pollutants, especially in water treatment techniques for removing heavy metals due to the porous structure of zeolites and other special features **(Veena *el al.*, 2021)**.

MATERIALS AND METHODS

Methyl methacrylate provided by (P.D.H). Absolute Ethanol (B.D.H), PVAprovided by (SIGMA), ($CrCl_3.H_2O$, $MnCl_2.4H_2O$, $FeCl_3$, $CoCl_2.6H_2O$, $NiCl_2.6H_2O$, $CuCl_2.2H_2O$, $ZnCl_2$, and $CdCl_2.H_2O$) provided by (B.D.H).

Instruments

Melting points of the synthesized compounds were measured by GMMallenKampm. MF-370 devised electro-thermal at the University of Baghdad, College of Sciences for Women. Fourier Transform Infrared (FTIR) spectra were obtained using a SHIMADZUE FT-IR 8400S Fourier transform within the wavenumber region between 4000 - 400 cm^{-1} using a KBr disc

and 4000 - 200 cm^{-1} using a CsI disc. electronic spectra for compounds in the (UV-Visible) region (200-1100) nm were recorded using a SHIMADZUE 1800 Double Beam UV-Visible spectrophotometer at the University of Baghdad. ^{1}H-NMR was performed using a Bruker Ultra Shield 500 MHz at Tehran University, Iran. Thermal analyses (TGA) of samples were performed under nitrogen atmospheres at 25˚C-900˚C and a heating rate of 20˚C/min using STA500 Germany in Tehran University, Iran. Molar conductivity measurements ($\mu s.cm^{-1}$) for metal complexes (10^{-3} M) in Ethanol at room temperature were carried out using LASSCO Digital Conductivity Meter. Magnetic moments (eff. B.M) for the prepared complexes in the solid state at room temperature were measured according to Faraday's method using Bruker Magnet B.M-6.

Synthesis

Synthesis of copolymer [methyl (S)-5-hydroxy-2, 2-dimethylhexanoate] (PMMA-PVA) ligand

In around-bottomed flask with a constant oxygen stream in an inert atmosphere of nitrogen, the (PMMA-PVA)-copolymer prepared by dissolving (1g, 0.01 mol) of polyvinyl alcohol (PVA) in a mixture of (2.5ml: 12.5ml) of absolute ethanol and deionized water in the presence of (0.5 g) from ammonium persulfate (APS) as a radical initiator which dissolved in 2ml of water with continuously stirring at room temperature (25^{o}C) then adding (1g, 0.01 mol) of methyl methacrylate; the mixture was refluxed at 70-80°C for 2.5 hrs in a water bath. Then the pink product was dried at room temperature for a whole night before being washed with diethyl ether (Scheme 1).

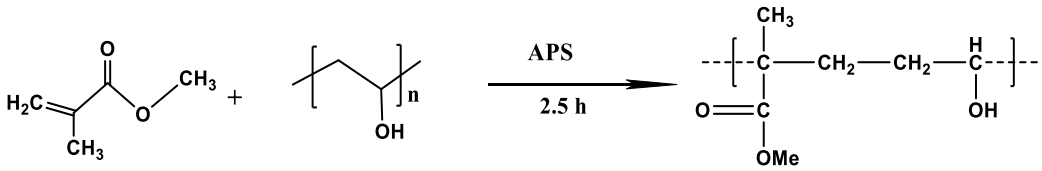

methyl metha acrylate **poly vanyl alcohol (PVA)**

methyl (*S*)-5-hydroxy-2,2-dimethylhexanoate
Chemical Formula: $C_9H_{18}O_3$
Molecular Weight: 174.2

(PMMA-PVA)

Scheme (1): Preparation of Polymethylmetha acrylate –PVA (PMMA-PVA) ligand

Synthesis of [methyl-5-hydroxy-2, 2-dimethylhexanoate] (PMMA-PVA) ligand complexes

To prepare ligand-complexes of poly Methyl methacrylate-PVA (PMMA-PVA) at a ratio of 2:1 from ligand to metal, (0.0576 g, 0.002 mol) of the ligand was dissolved in (5 ml) of distilled water and (20 ml) of absolute ethanol with continuous stirring in a condensation flask until it dissolved. The corresponding weight of (0.001 mol) metal salt dissolved in (10 ml) of absolute ethanol was added. The mixture was refluxed with continuous stirring at 45°C for 3hrs. The product was placed in a watch glass and let dry at room temperature.

RESULTS AND DISSCUSIONS

FTIR Spectra

Specific vibrations of chemical bonds or functional groups within molecules were reflected as peaks in FTIR spectra **(Mathur *el al*.,2018)**. It is shown in Figure 1 that KBr FTIR spectroscopy in the range of 4000-400 cm^{-1} and CsI FTIR spectroscopy in the range of 4000-200 cm^{-1} were used to determine the experimental and theoretical structure of the (PMMA-PVA) polymer complexes. Experimental FT-IR showed a distinctive band of the -OH functional group in the range of 3446-3213 cm^{-1} in the IR spectra of the compounds, suggesting its nonparticipation in coordinate bond formation towards all metal ions. Furthermore, as shown in Figure 1. b, the peak's width expanded after coordination. This may be due to moisture in the sample or complexes containing coordinated water molecules **(Abdi *el al*., 2020; Anacona *el al*., 2021)**. Other stretching bands were found at 1701-1616 cm^{-1} for υ(C=O) carboxylic of ester **(Nabeel *et al*., 2022; Tabarek & Ahlam 2023)**. The loss of the C=O signal, originally at 1616-1650 cm^{-1}, was consistent, providing strong evidence for the coordination of Ligand (PMMA-PVA) towards the central metal ion, Figure 1. Table 1 shows that the typical peak at ~1700 cm^{-1} for compounds containing the (C=O) ester group relocated to 1600 cm^{-1}**(Muna *et al*., 2022)**. In complexes, the carbonyl group was weakened after bonding due to creating a coordination bond between the oxygen of the C=O group and the central metal ion, as indicated by the peak displacement.

Table (1): The FT-IR spectrum of the synthesized ligand and its complexes.

Comp.	υ(OH)	υ(COO) ester	υ(C-OCH_3)	υ(CH-CH_2)	υ(M-O)	υ(M-Cl)	Others.
L	3444	1701	1147	2987-2879	-		
CrL	3434	1647	1124	2921-2871	599	335	w H_2O = 910 ρ OH =846
MnL	3446	1622	1118	2947-2860	559	329	w H_2O = 984 ρ OH =833
FeL	3429	1623	1118	2929-2873	597	327	w H_2O = 997 ρ OH =864
CoL	3438	1649	1083	2925-2856	557	316	w H_2O = 983 ρ OH =846
NiL	3240	1616	1095	2927-2854	567	324	w H_2O = 987 ρ OH =827
CuL	3417	1714	1101	2948-2873	549	335	w H_2O = 927 ρ OH =846
ZnL	3240	1620	1095	2927-2856	567	331	w H_2O = 983 ρ OH =881
CdL	3213	1650	1101	2950-2875	520	329	w H_2O = 987 ρ OH =875

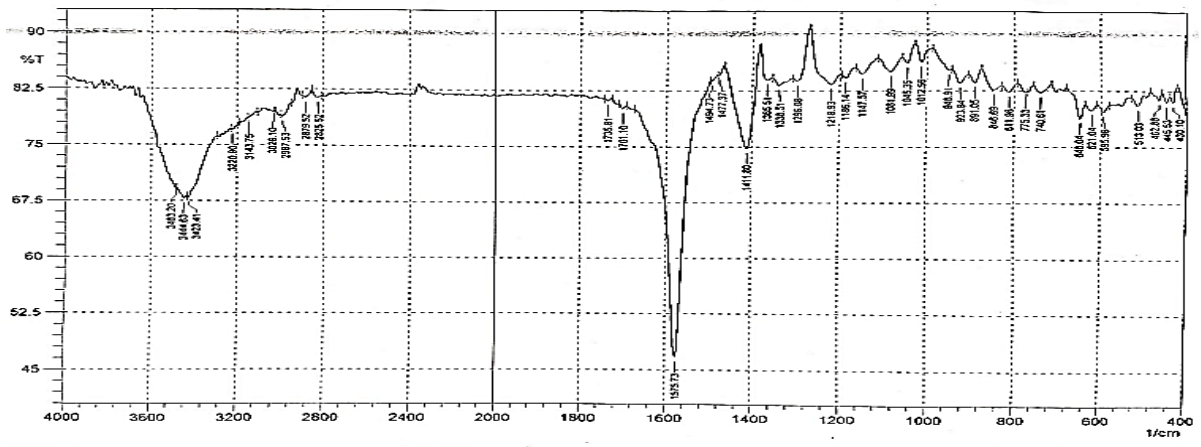

A

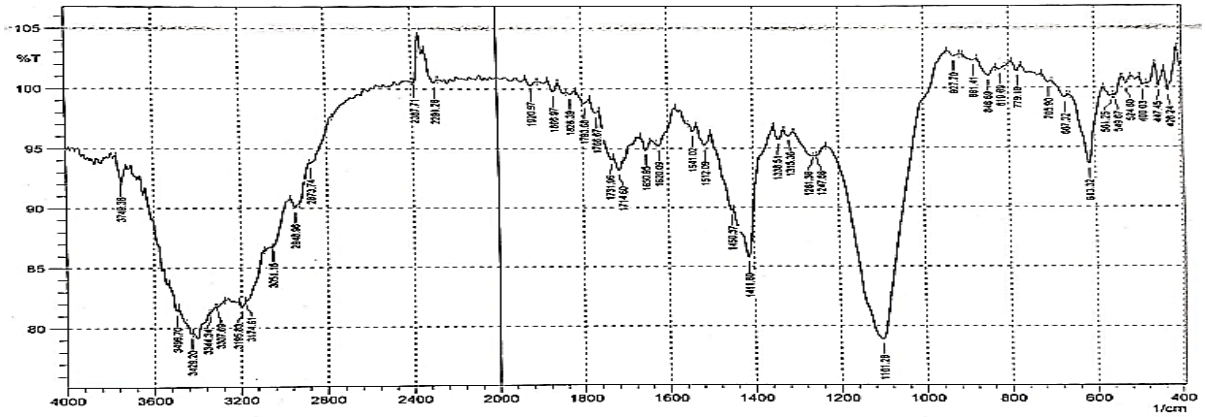

B

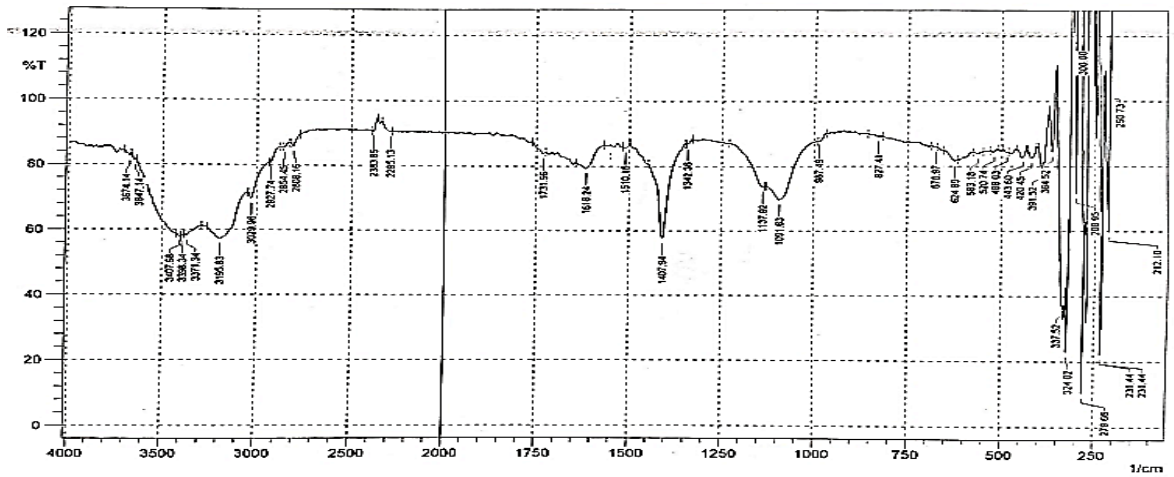

c

Figure (1): The FTIR Spectra for (a) PMMA-PVA -L (b) NiL (c) CuL

The Electronic spectra, (UV-Vis) of ligand and its complexes:

Intense absorption at (323) nm (20661) cm^{-1} in the UV-Vis spectrum of (PMMA-PVA)-ligand was ascribed to the (n→π*) transition, while intense absorption at (229) nm (43668) cm^{-1} was ascribed to the (π→π*) transition, Figure 2. Table 3 contains information about the spectra, molar conductivity, and magnetic moments of all metal complexes of the (PMMA-PVA)-ligand in ethanol for MnL, FeL, CdL complexes and in DMSO for CrL, CoL, NiL, CuL, and ZnL complexes.

Where three bands of complexes were uncultivated: Three bands, corresponding to $^6A_1g\rightarrow{}^4T_1g$ (G), $^6A_1g\rightarrow{}^4T_2g$ (G), and $^6A_1g\rightarrow{}^4A_2g$+Eg (G) were seen for the Mn (II)-PMMA-PVA complex at 12468, 20080 and 28248 cm^{-1} respectively (**Al-Issa *el al*., 2017)**.

Co (II)-PMMA-PVA complex showed three bands in the visible region with an average of 14749cm^{-1}. This value which assigned to transition $^4T_1g\rightarrow{}^4T_2g$ (F) **(Nuha&Naser, 2023)** and a value with an average of 16260 cm^{-1} for $\upsilon^4T_1g\rightarrow{}^4T_1$ (P) while $^4T_1g\rightarrow{}^4A_2g$ appeared at 17211 and it forbidden transition Scheme 2(a).

The spectrum of Cr (III) complex olive showed three absorption bands at (619, 451, and 259) nm (16155, 222172, and 38610) cm^{-1} assigned to $^4A_2g\rightarrow{}^4T_2g$, $^4A_2g_{(F)}\rightarrow{}^4T_1g$ and $^4A_2g_{(F)}\rightarrow{}^4A_2g$ transitions, suggesting an octahedral geometry **(Sahar *el al*., 2020; Rasha& Abbas, 2023).)**.

The Fe (III) complex spectrum showed three bands at 682, 590, 416 nm (14662, 16949, 24038) cm^{-1} assigned to $^6A_1g\rightarrow{}^4T_1g$,$^6A_1g\rightarrow{}^4T_2g$, and $^6A_1g\rightarrow{}^4A_1g$ +^4Eg respectively. Transition at 336 nm (29776) cm^{-1} attributed to C.T (LMCT) and that suggesting an octahedral geometry **(Anum *el al*., 2022** the magnetic moment value is 5.6 BM, Scheme 2(c).

For Ni(II) complex spectrum showed three bands at (920, 769, 502, 385, and 290) nm (10809, 13003, 19920, 25974, and 34482)cm^{-1} assigned to $^3A_2g\rightarrow Eg$, $^3A_2g\rightarrow{}^3T_2g$,$^3A_2g\rightarrow{}^3T_1g_{(F)}$ and $^3A_2g\rightarrow{}^3T_1g_{(P)}$ transition, respectively; the magnetic moment value is 2.3 BM suggesting an octahedral geometry **(Sahar *el al*., 2018*;* Veyan *el al*., 2020)** , Scheme 2 (b)

Cu (II) complex spectrum showed one band at 920nm (10869) cm^{-1}, assigned to $^2Eg\rightarrow{}^2T_2g$ and C.T transition; the magnetic moment value is 1.2 BM suggesting an octahedral geometry, Scheme1 (a) **(Sahar *el al*., 2021)**.

Finally, the magnetic moment value is diamagnetic for both Zn (II) and Cd (II) complexes (ZnL) and (CdL), which is attributed to metal to ligand charge transfer, but the spectra show no d-d electronic transitions in the visible region. The absorption bands are 505 and 498 nm (34364, 20080) cm^{-1} **(Haneen & Sahar, 2022)**. Scheme1(a)

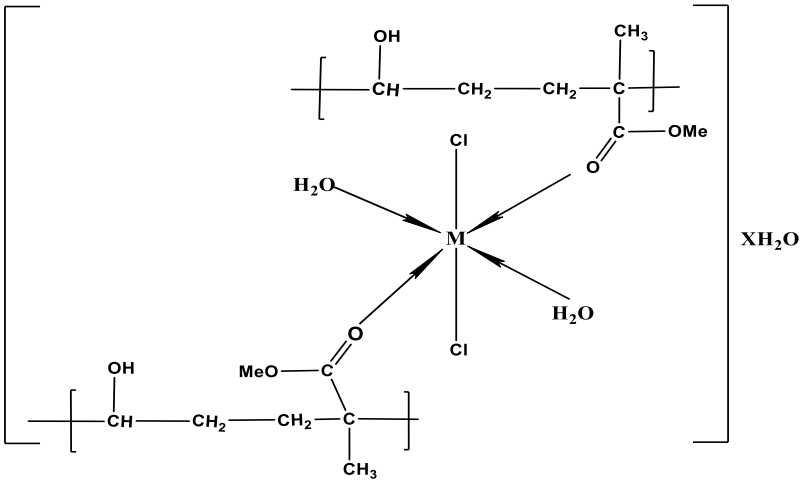

(a) M= Mn, Cu, Zn, Cd, Co

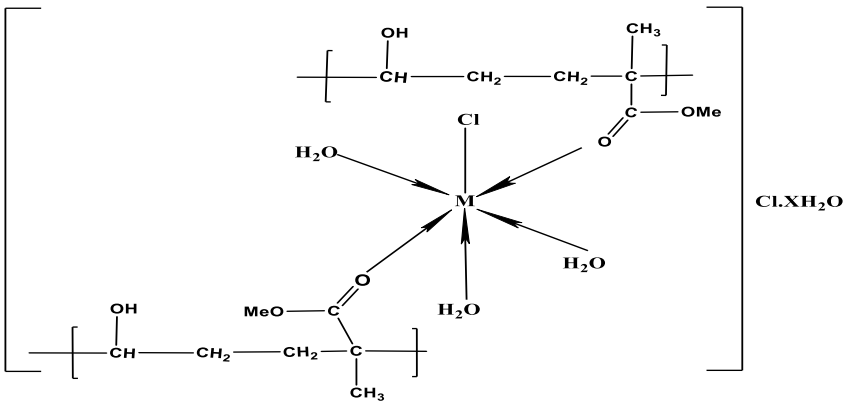

(b) M= Ni

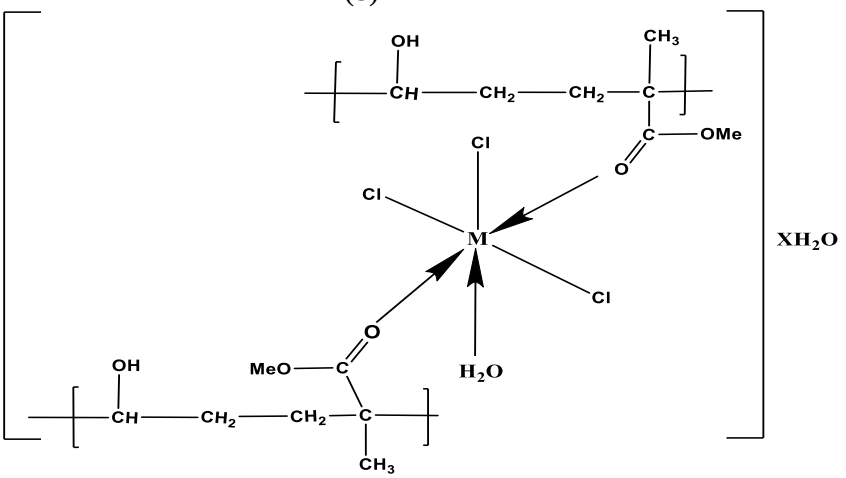

(c) M=Cr,Fe

Scheme (2). The geometrical structure of a. Octahedral [ML_2 (Cl_2)]. XH_2O b. Octahedral [ML_2Cl] Cl.XH_2O c. Octahedral [ML_2Cl_3].XH_2O

Table (2): Electronic spectra, spectral parameters, molar conductivity, and μ*eff* of L- metal complexes.

Comp.	λnm	ῡcm-	Assignments	Molarcond.	μeff(B.M)	Structure
L	323	30959	n→π*			
	229	43668	π→π*			
Cr-L	619	16155	4A2g→4T2g	6.1	3.7	Octahedral
	451	22172	4A2g→4T1g			
	397(cal.)	25188	4A2g→4T1g			
	259	38610	Intra ligand			
Mn-L	802	12468	6A1g→4T1g(G)	27	5.2	Octahedral
	498	20080	6A1g→4T2g(G)			
	354(cal.)	28248	6A1g→4A2g+4Eg(G)			
	275	36363	Intra ligand			
Fe-L	682	14662	6A1g→4T1g	17.3	5.6	Octahedral
	590	16949	6A1g→4T2g			
	416(cal.)	24038	6A1g→4A1g+4Eg			
	336	29776	C.T (LMCT)			
	266	37594	Intra ligand			
Co-L	678	14749	4T1g→ 4T2g (F)	11.5	5.3	Octahedral
	615	16260	4T1g→4T1g(P)			
	581	17211	4T1g →4A2g			
	275	36363	Intra ligand			
Ni-L	920	10869	3A2g→Eg	42	2.3	Octahedral
	769	13003	3A2g→3T2g			
	502	19920	3A2g→3T1g(F)			
	385	25974	3A2g→3T1g(p)			
	290	34482	Intra ligand			
Cu-L	920	10869	2Eg→2T2g	8.9	1.2	Octahedral
	296	33783	C.T			
	209	47846	Intra ligand			
Zn-L	505	34364	C.T	17.3	Diam.	Octahedral
	268	28571	Intra ligand			
Cd-L	498	20080	C.T	3.5	Diam.	Octahedral
	286	33223	Intra ligand			

Table (3): Physical properties of the ligand and its complexes.

Compounds	M.p°C (dec) °C	Color
L	180-182	Pink
FeL	190-192	Yellow
CuL	138-140	greenish yellow
MnL	170-172	Pink
CdL	188-190	Off-white
CrL	248-250	Olive
NiL	198-200	Yellow
CoL	240-242	turquoise
ZnL	230-232	Light Pink

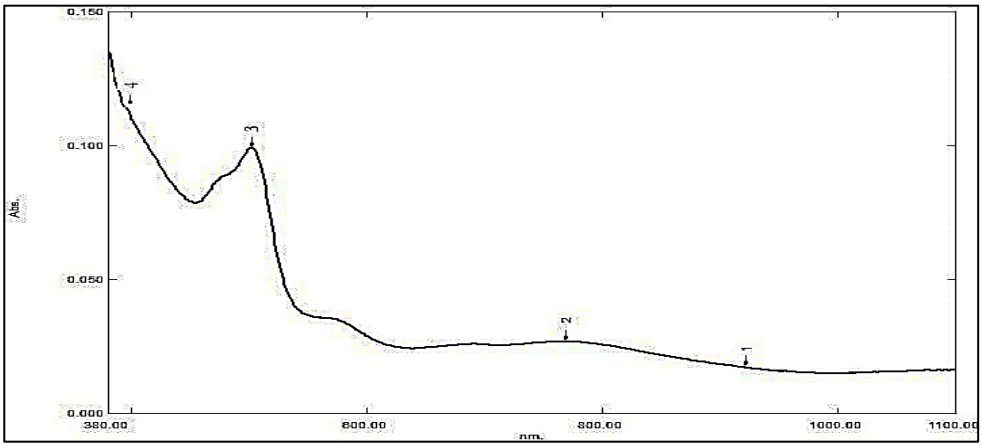

(a)

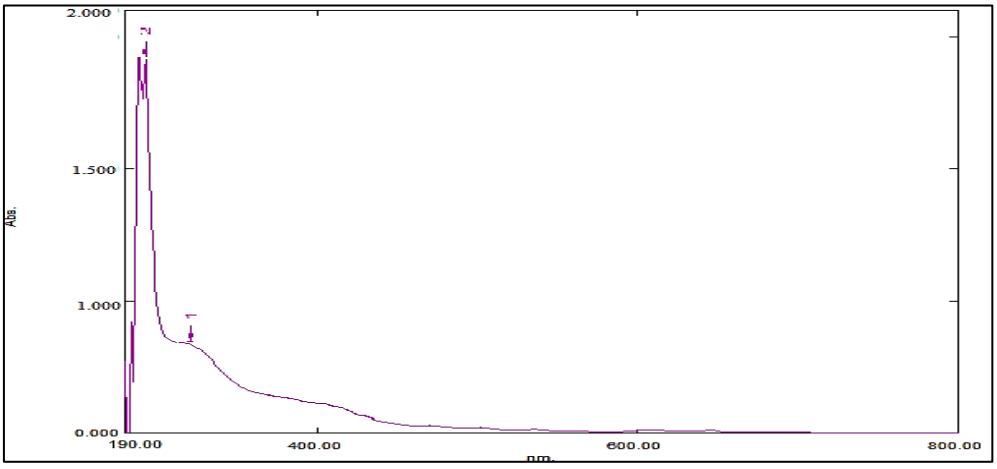

(b)

Figure (2): Electron spectrum of a. (PMMA-PVA) ligand b. NiL complexe

HNMR spectrum

Nuclear magnetic resonance spectroscopy (1HNMR) is essential for studying substances and their structures. The ^{1}H-NMR technique was used to characterize the synthetic polymer. Figure 3 and Table 4 showed that the methyl and methylene protons in the PMMA-PVA structure correspond to a signal at 1.16–1.8 ppm and 2.0–2.5 ppm, respectively. The peaks at δ 3.61-3.92 ppm were identified as protons for the methylene group. The Proton of the hydroxyl group was identified as the source of the peak at δ 10.83 ppm **(Haroon *el al.*, 2021)**. The presence of the Methyl methacrylate chain, and hence the occurrence of polymerization to generate the desired product, was confirmed by the ^{1}HNMR spectrum.

Table (4): ^{1}H NMR spectral data of L-PMMA-PVA and CrL complexe

Chemical shifts (ppm)	Assignments in DMSO
1.16 - 1.8 ppm and 2.0 - 2.5 ppm	methyl and methylene protons
3.61 - 3.92ppm	protons for methylene group
10.83 ppm	Hydroxyl group proton (OH)

(a)

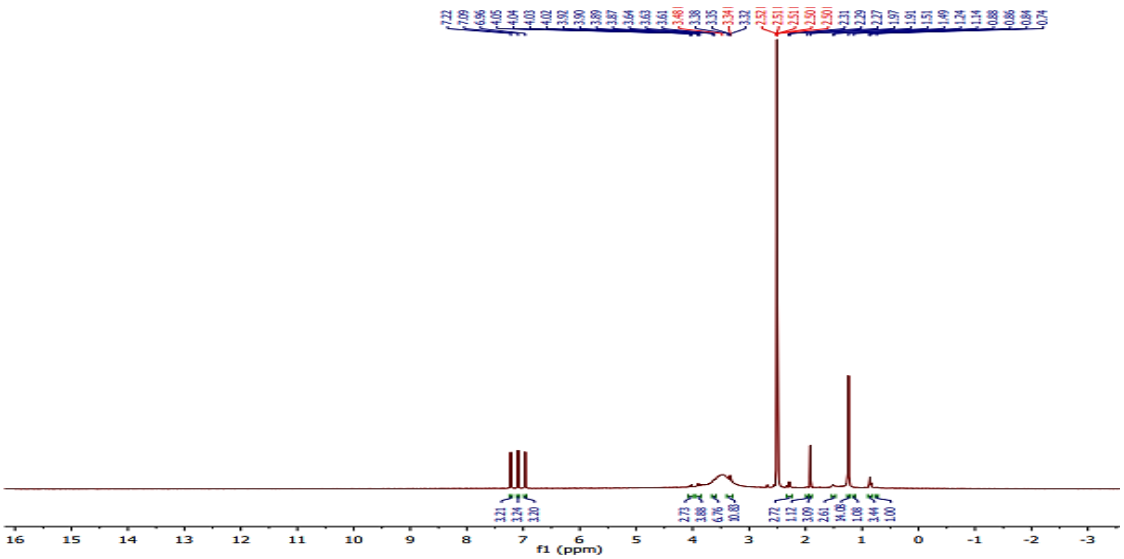

(b)

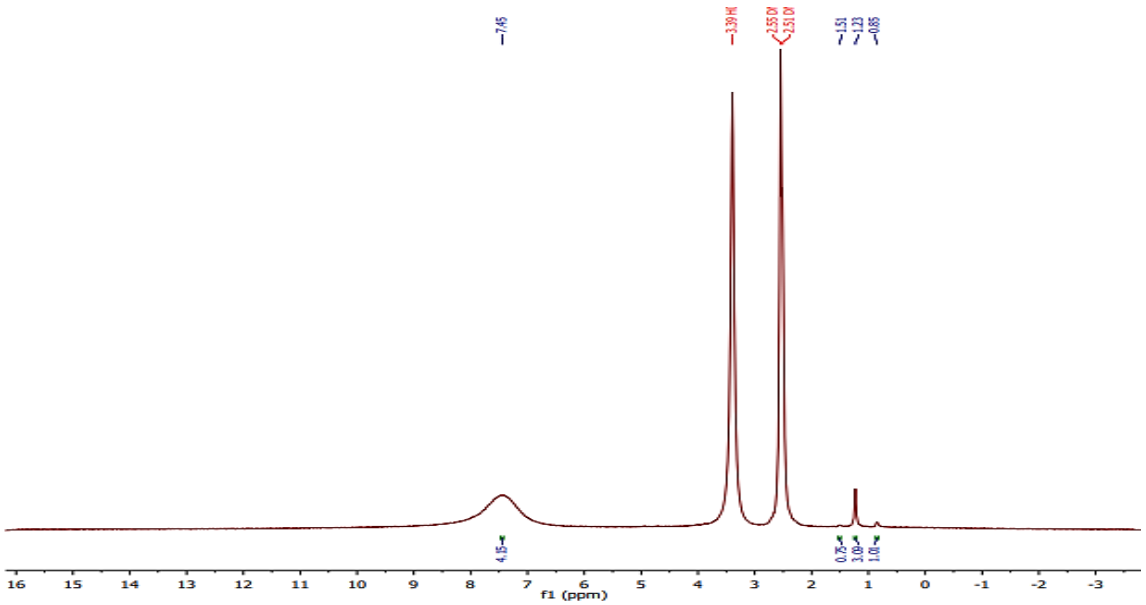

Figure (3): HNMR spectrum of (a) L (PMMA- PVA) and (b) CrL

Thermal Gravimetric Analysis (TGA)

Thermogravimetric analysis (TGA) was used to understand the effects of temperature and time on the weight of polymeric materials. Polymeric materials can undergo weight changes due to decomposition, oxidation reactions, and physical processes, including sublimation, evaporation, and desorption **(Dilkes *el al.*, 2019)**. TGA-curve of two (PMMA-PVA)-complexes as illustrated in Figure 4 and Table 5. Thermal stability of Cr and Fe complexes studied by TGA. The TGA tests were performed at ~30 ºC to 900 ºC. The CrL complex was shown to be disassembled into three parts in Figure 4.a. First, a small loss of 10.31% from total mass when compared to a temperature of 110C suggests that water molecules were evaporated from the sample. The polymer (ligand) chains, CO_2, CO, and Cl fragments caused a 40.34% weight loss when heated to around 625ºC. The remaining complex lost 7.8% of its mass upon decomposing from 625-900 ºC **(Ashok *el al.*, 2020)**. The degradation of polymer residues for the coordinated ligand molecules accounted for the modest increase in degradation observed compared to the previous stage. Upon further heating, the polymer chains and metal oxide residue were left as the final residue at 41.55 %. Almost similar changes were observed in the FeL complexe TGA curve (Figure 4. b). However, the intermediate residue stability was less than the CrL complex, which gradually decomposed in three stages. The loss of water molecules results in (9%) at about 130 ◦C. The second weight loss of 49% was observed at 631 ◦C, again due to the first weight loss along with the polymer chains and CO_2, CO, and Cl as gases from the ligand (PMMA-PVA) Scheme 3. The residue of polymer (ligand) chains and the Fe^{+3} oxides contributed nearly 31.16 %. Our results were supported by previous knowledge of the stabilities of other complexes containing these transition metals **(Neha *el al.*, 2018; Wu *el al.*, 2003)**.

Table (5): Thermal analyses data for CrL and FeL.

Comp.	Dissociation stages	Temp range in °C	Weight loss found %	Weight loss (Cal.) %	Final Weight residue found %	Final Weight residue (cal.) %
CrL	StageI StageII StageIII	20-150 150-625 625-900	14.42 36.21 7.8	5 48 5	41.55	42 it represent residue of polymer and metal oxide
FeL	StageI StageII StageIII	20-126.05 126.05-631.81 631.81-900	9 49.5 10.35	8.61 49.9 10.34	31.16	31.15 it represent residue of polymer and metal oxide

(a)

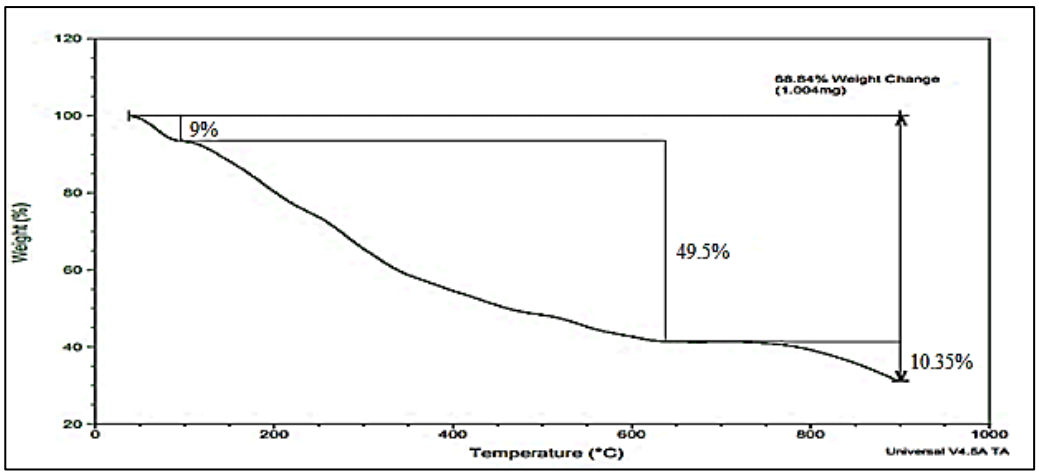

(b)

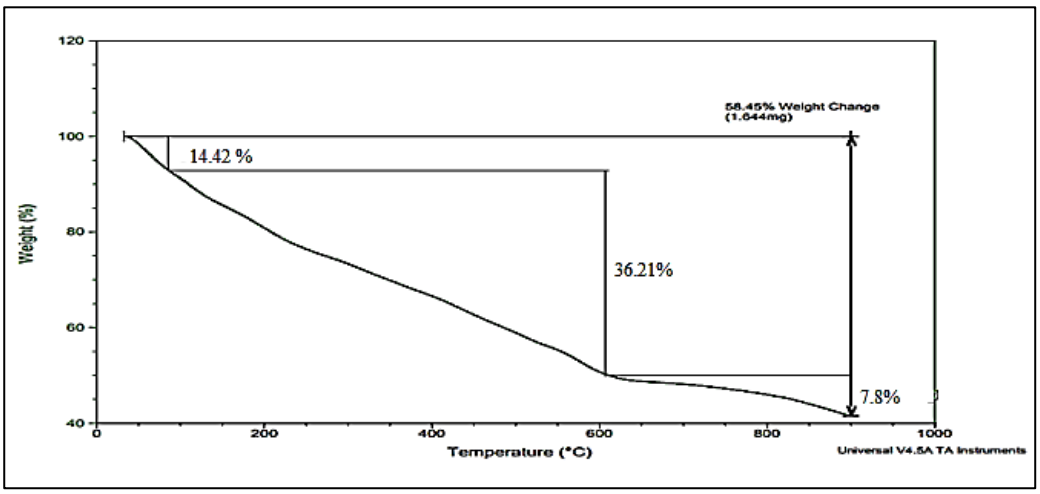

Figure (4): TGA analysis for: (a) CrL and (b)FeL

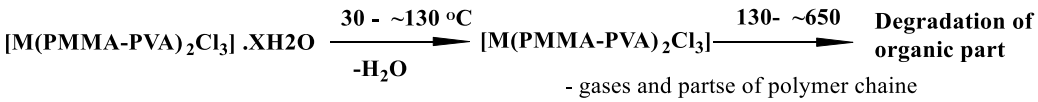

M= Cr or Fe

Scheme (3): Thermal behavior of CrL and FeL complexes.

XRD analysis

X-ray diffraction helps investigate nanoparticles **(Peighambardoust *et al.*, 2020)**. which were performed on a category of ligands. The sharp peaks demonstrated the Nanoscale feature of Cu(II) and Fe(II) complexes. Comparatively distinct peaks at 2Θ (16, 18.5, 22, 33, 34, and 41) were observed for the CuL Nano complex, but for the FeL Nano complex, the spectra were entangled, and the unique peaks vanished. Probably, X-ray spectroscopy cannot figure it out because of the shielding effect of the represented ligand-polymer molecules **(Siva *el al.*, 2019)** Figure 5.

(a)

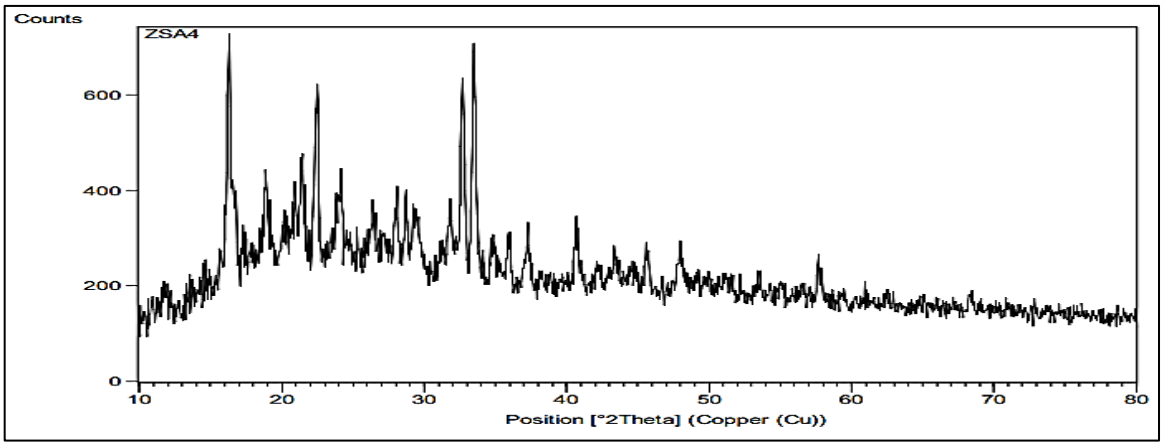

(b)

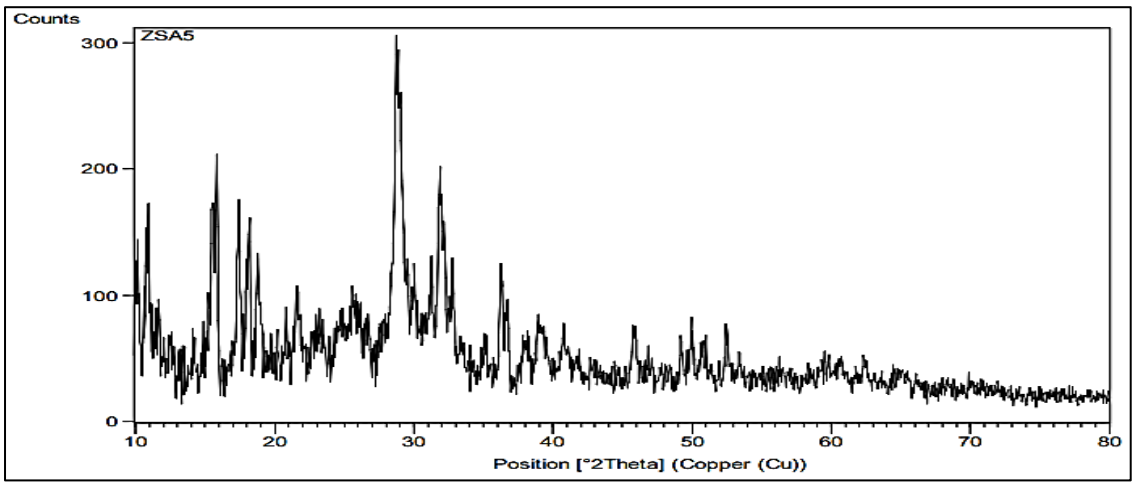

Figure (5): XRD patterns of a. CuL Nano complex b. FeL Nano complex.

Atomic Force Microscopy (AFM)

The method measures the forces exerted by a sharp cantilever tip on a surface at a very close distance, yielding two- and three-dimensional surface profiles at the nanoscale. The 3D and two-dimensional pictures of nano (CuL and FeL) complexes are shown in Figure 6. The granularity accumulation distribution charts for these complexes were displayed and shown in Figure 7. The average diameters and ten hight of CuL and FeL nano complexes particles were displayed in Table 6, with a mean diameter ranging from (4.5-9.0 nm) and an average diameter of 82.96 nm. The diameters of the particles making up FeL nano complex range between (20-45 nm), with an average diameter of 97.74 nm.

Table (6): Summary of the AFM information for CuL and FeL nano complexes

Sample	Roughness Averege (nm)	Root Mean Square (nm)	Average Hight (nm)	Average Diameter (nm)
CuL	1.31	1.73	6.89	82.9
FeL	8.3	10.3	42	97

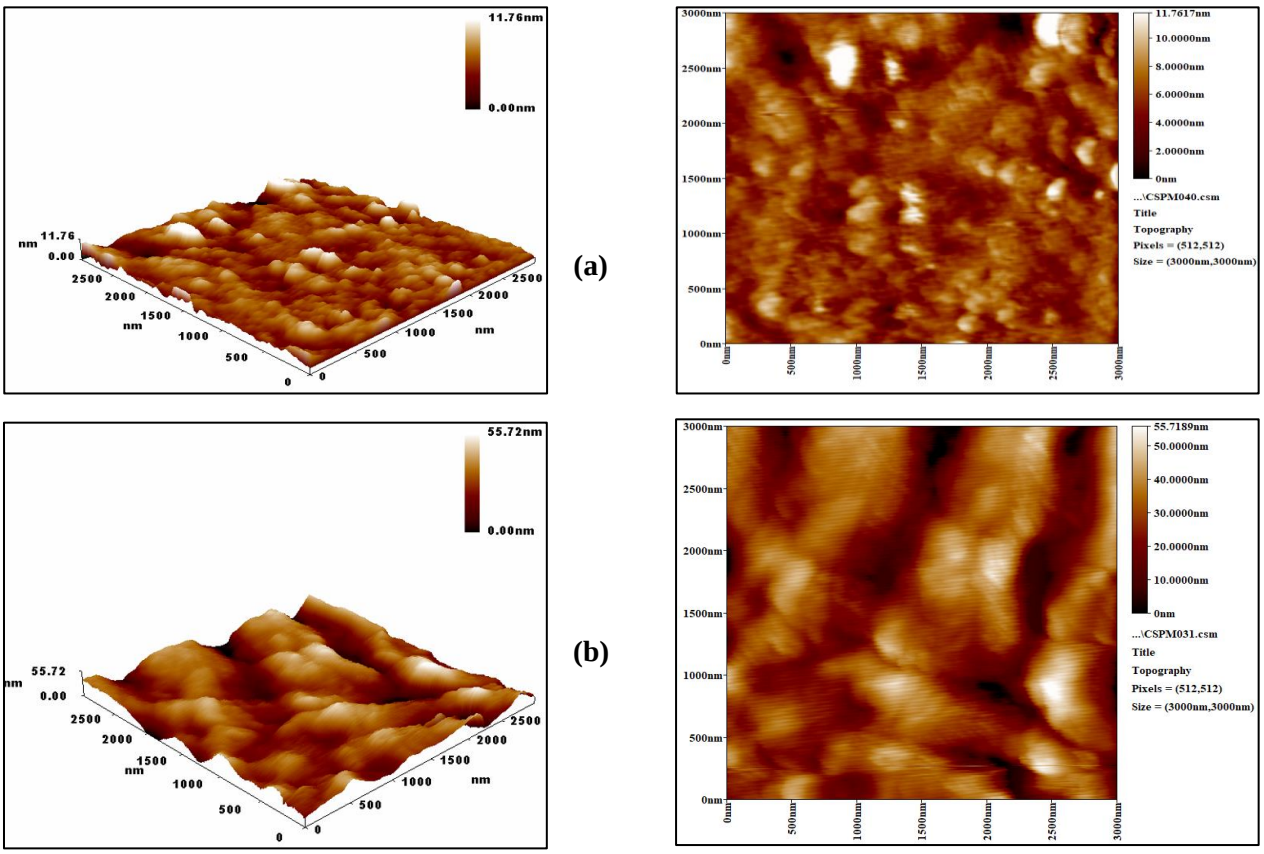

Figure (6): AFM three and two-dimensional image for (a) CuL (b) FeL nanoparticles complexes

(a)

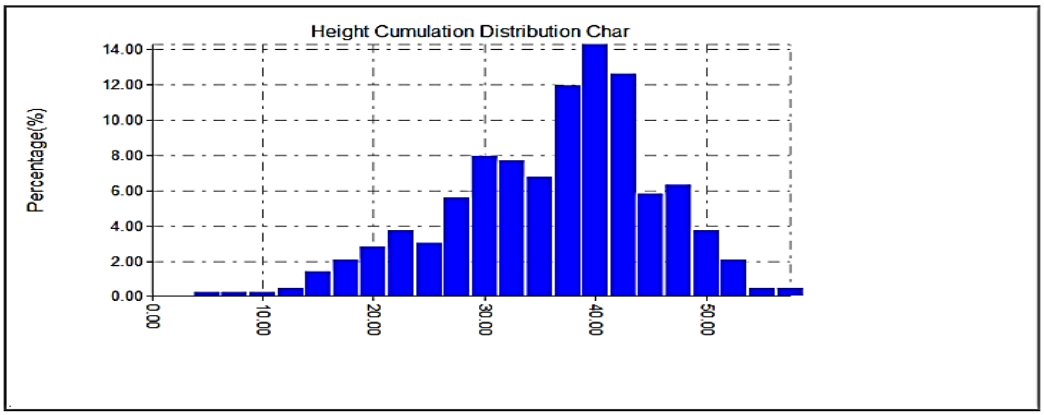

(b)

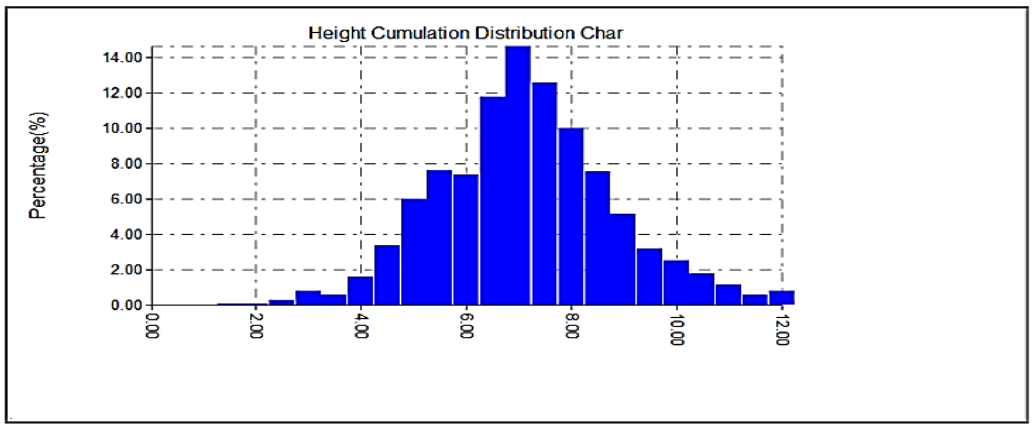

Figure (7): Granularity accumulation distribution of (a) CuL (b) FeL nanoparticles complexes.

(SEM) Scanning Electron Microscopy and Energy Distributed X-Ray Spectrometry (EDS)

Pictures of the CuL Nano complex taken using a scanning electron microscope (SEM) reveal particles with sizes ranging from around (20-55nm), Figure 8. Similar results are seen for the FeL Nano complex; scanning electron microscopy (SEM) pictures of the FeL Nano complex were also displayed, revealing particle sizes of around (35-46nm).

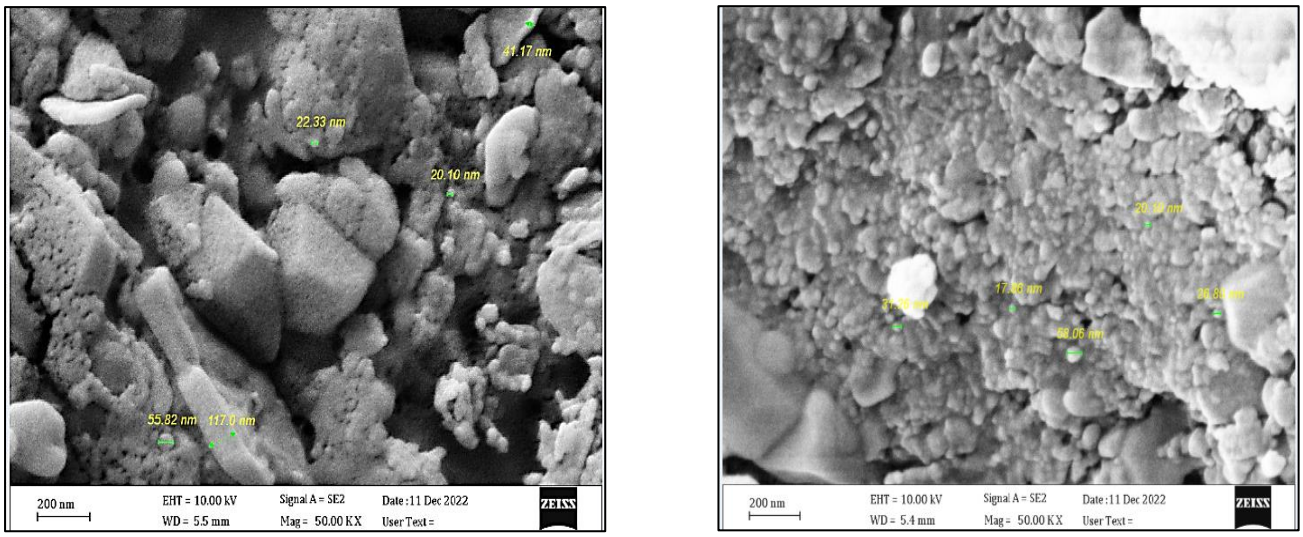

(a) **(b)**

Figure (8): SEM of (a) CuL (b) FeL nanoparticles complexes.

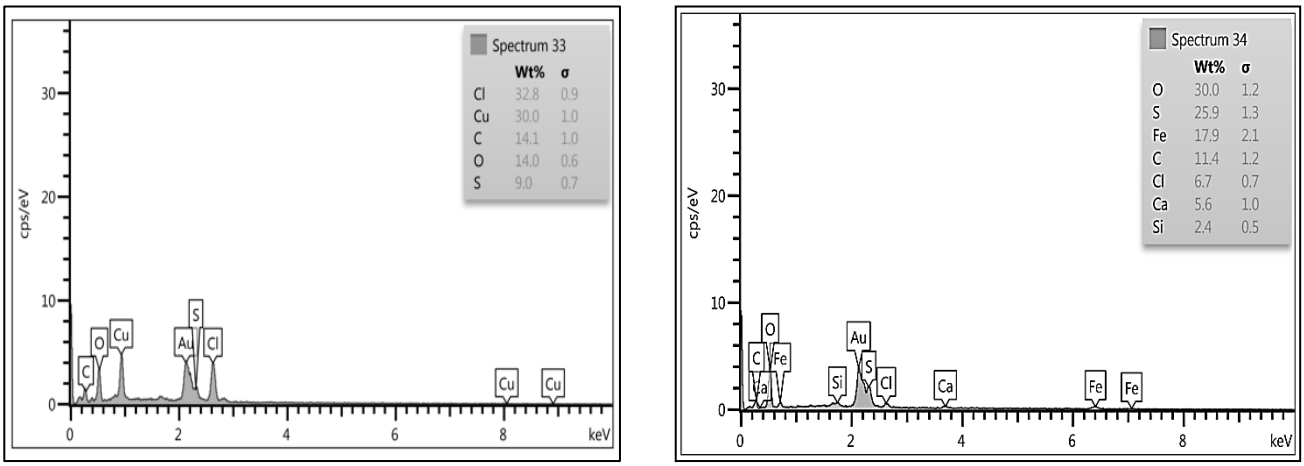

(a) **(b)**

Figure (9): EDSof (a) CuL (b) FeL nanoparticles complexes.

Application of PMMA-PVA to remove elements from contaminated water.

Traditional and membrane approaches are available for removing heavy metal pollutants from wasted streams. Contaminated heavy metals must be recovered to prevent further contamination and gain economic benefit.

An internal standard method (In) and a multi-standard calibration method were used to precisely analyze metals in water samples **(Husam *el al.*, 2013; Maysoon *et al.*, 2022)**.

PMMA-PVA was applied to remove some of the elements in polluted water that were left over from the power stations, where very trace concentrations of the elements that were previously detected in the samples taken from the liquid waste left over from two power

stations were prepared, which are (20, 40, and 60) ppm, using the atomic absorption technique to determine its percentage after the removal process, which conducted through the preparation of a polymeric composite of each of the prepared PMMA-PVA and zeolite. The obtained results are listed in Table (7).

Table (7): The experimental result of removal metals (Mn(II), Fe(III), Ni(II) and Cu(II)) by designed PMMA-PVA - composite.

Metal	Initial concentration ppm.	Final concentration (after applying PMMA-PVA) ppm.	Final concentration (after applying PMMA-PVA with composite at 40 ppm from each metal)	Concentration ppm. (in the wastewater from Al Doraa power station after application PMMA-PVA with composite)	Concentration ppm. (in the wastewater from South of Baghdad power station after application PMMA-PVA with composite)
Mn(II)	20	4	0.9	0.95	0.54
	40	10			
	60	37.5			
Fe(III)	20	4.5	ND	ND	ND
	40	10			
	60	17.5			
Ni(II)	20	2.8	0.27	0.23	0.06
	40	17			
	60	38			
Cu(II)	20	15	0.088	0.16	0.06
	40	20			
	60	44			

CONCLUSION

The findings point to the potential for producing Nanocomposites by complexation of polymeric ligand methyl(S)-5-hydroxy-2-methylhexanoate (PMMA-PVA) with metals that were only partially soluble in solvents like water, ethanol, and DMSO. Because of the copolymer's fast complexation with elements, this property of the (PMMA-PVA) copolymer allows for its wide range of use.

Complexation and adsorption are two mechanisms by which it successfully purges water of harmful substances, wherein one approach involves ligand-to-metal interactions in polluted water. In contrast, in the adsorption method, composites were made by combining zeolite and poly (Methyl methacrylate-co-polyvinyl alcohol) or (PMMA-PVA). Examination of polluted water before and after using the produced compounds revealed that the removal utilizing the composite materials was significantly more effective, with the concentration being recorded as very low and the concentrations of some metals completely disappearing from polluted water.

REFERENCES

1. Abdi, Y., Bensouilah, N., Siziani, D., Hamdi, M., Silva, A.M.S., &Boutemeur, K. B. (2020). New Complexes of Manganese (II) and Copper (II) Derived from the Two New Furopyran-3, 4-Dione Ligands: Synthesis, Spectral Characterization, ESR, DFT Studiesand Evaluation of Antimicrobial Activity. *Journal Molecules Structure*, *1202*, 127307.
2. Abdullah, A. B., Muhammad, H. A., & Tawfik, A. S. (2021). Poly (acrylamide acrylic acid)/Baghouse dust magnetic composite hydrogel as an efficient adsorbent for metals and MB; synthesis, characterization, mechanism, and statistical analysis. *Sustainable Chemistry and Pharmacy*, 23, 100503.
3. Al-Issa, MA, Abbas, AA, & Matty, FS. (2017). Synthesis and characterization of Schiff base derived fromchitosan and its complexes with (Co^{+2}, Ni^{+2} and Cu^{+2}). *Ibn AL-Haitham Journal Pure Application Science*, 29(2), 115–29.
4. Anacona, J.R., Santaella, J., Al-shemary, R.K.R., Amenta, J., Otero, A., Ramos, C., & Celis, F. (2021). Ceftriaxone-Based Schiff Base TransitionMetal(II) Complexes.Synthesis, Characterization, Bacterial Toxicity, and DFT Calculations.Enhanced Antibacterial Activity of a Novel Zn(II)Complex against *S.aureus* and *E.coli*. *Journal Inorganic Biochemistry*, *223*, 111519.
5. Anum, H., Mohammad, S.Iqbal, Naveed, A., Nabil K. A. & Atta U. R. (2022) Fe (III)-Rhamnoxylan—A Novel High Spin Fe (III) Octahedral Complex Having Versatile Physical and Biological Properties. *Polymers*, 14, 4290.
6. Ashok,K. B., Somnath, P. L., & Kafeel, A. S. (2020). A Novel Mixed Ligand Zn-Coordination Polymer: Synthesis, Crystal structure, Thermogravimetric analysis and Photoluminescent Properties. *Inorganica Chimica Acta*, 500, 119219.
7. Ashvinder, K. R., Vijai, K. G., Adesh, K. S., Stefan, I. V., Magda, H. A., & Vijay, K. T. (2021). Water desalination using nanocelluloses/cellulose derivatives-based membranes for sustainable future. *Desalination*, 520, 115359.
8. Balbir, S. K., Anjal, S., Ami, K.S., & Dhiraj, S. (2021). Hydrogels Synthesis, Classification, Properties and Potential Applications. *Journal of Polymers and the Environment*, 29, 3827-3841.
9. Carrasco, S. V., Vimirgiotis, M.J., & Santos L.S. (2009). The Morita-Baylis-Hillman Reaction: Insights into Asymmetry and reaction Mechanisms by Electrospray Ionization Mass Spectrometry. *Molecules*, 14, 3989-4021.
10. Dilkes H L, Lant P A, Laycock B, & Pratt S. (2019). The rate of biodegradation of PHA bioplastics in the marine environment: A meta-study. *Marine Pollution Bulletin*, 142, 15–24.
11. Haneen, R. A., & Sahar, S. H. (2022). Preparation and study of the physical properties of some complexes with Schiff base ligand for cefdinir derivative. *Iraqi Journal of Market Research and Consumer Protection*,14(2), 110-120.
12. Husam, M., Mutaz, Al-Q., Mahmoud, A. K., & Fuad, Al-R. (2013). Determination of Different Trace Heavy Metals in Ground Water of Southwest Bank/Palestine by ICP/MS. *Journal of Environmental Protection*, 4, 818-827.
13. Karmen, M., & Anamarija, F. (2022). *Zeolites - From Discovery to New Applications on the Global Market*. *WEB OF SCIENCE*, p. 4, Croatia.
14. Luciano, F.D. M., Gilberto, R. &Antônio, E. C. P. (2022). Zeolite Application in Wastewater Treatment. *Adsorption Science &Technology*, 2022, 26-52.

15. Mahmoud, M.E., Ebtissam, A. S., Mohamed, A. S., & Mohamed, S. A.(2020) Removal of radioactive cobalt/zinc and some heavy metals from water using diethylenetriamine/2-pyridinecarboxaldehyde supported on NZVI. *Microchemical Journal*, 145, 12-32.
16. Mathur, N., Jain, N., & Sharma ,AK. (2018). Synthesis, characterization and biological analysis of some novel complexes of phenyl thiourea derivatives with copper. *Open Chemistry Journal*, 5(1), 182-195.
17. Maysoon, M. A., Sahar, S.H., & Ahmed K H. (2022). Comparative of Green-Synthesis of Bimetallic Nanoparticles Iron/Nickel (Fe/Ni) and Supported on Zeolite 5A: Heterogeneous Fenton-like For Dye Removal from Aqueous Solutions. *Asian Journal of Water Environment and Pollution*,19(5), 53-66.
18. Muhammad, H., Rooh, U., Sahid, M.,Fazal, H., & Naeemullah. (2021). Synthesis and Characterization of Starch-g-Poly Methyl methacrylate and Their Properties as Adsorbents for Removing Rhodamine 6G from Water. *Journal of Polymer Research*, 28, 330.
19. Muna, A. T., Sana, H. A. &Sura K. I. (2022). Synthesis and Characterization of new demulsifier from natural and synthetic polymer. *Iraqi Journal of Market Research and Consumer Protection*, 14(2),26-33.
20. Nabeel, H. A., Ali A., & Ali, J. A. (2022). Hyperbranched Polyester Polymer Preparation and Study Its Effect on Some Properties of Polypropylene. *Egyptian Journal of Chemistry*, 65(8), 35-43.
21. Neha,M.& Biplab,M. (2018).TGA Analysis of Transition Metal Complexes Derivedfrom Phenothiazine Ligands Introduction. *International Journal of ngineering & ScientificResearch*, *6*, 47-57.
22. Noreen, S., Pervaiz, F., Ijaz, M., & Shoukat, H. (2022). Synthesis and characterization of pH-sensitive chemically crosslinked block copolymer [Hyaluronic acid/Poloxamer -co-poly (Methacrylic acid)] hydrogels for colon targeting. *Polymer-Plastics Technology and Materials*, 61(10), 1071- 1087.
23. Nuha, A.A, & Naser, D. S. (2023). Synthesis Characterization, and Biological Activity of New Metal Io.n Complexes with Schiff Base (Z)-3((E)-2-Hydroxybenzylidene) hydrazineylidene) indolin-2-one. *Journal Medicinal and Chemical Science*, 6(7), 1660-1674.
24. Pishnamazi, M., Ghasemi, S., Khosravi, A., Zabihi, S., A., Hasan, Z.A., & Borghei, S. M. (2021). Removal of Cu (ll) from industrial wastewater using poly (acrylamide-co-2-acrylamide-2-methyl propane sulfonic acid)/graphene oxide/sodium alginate hydrogel: Isotherm, kinetics, and optimization study. *Journal of Water Process Engineering*, 42, 102144.
25. Rasha K. H. A., & Abbas A. S. A. (2023). Synthesis Characterization, and Thermal Analysis of a New Acidicazo Ligand's Metal Complexes. *Baghdad science Journal*, 20(1), 121-133.
26. Sahar S. H., Nidhal M. H., Shaymaa, R. B., & Asmaa, M. S. (2021). Biological evaluation and theoretical study of Bi-dentate ligand for Amoxicillin derivative with some metal ions. *Baghdad science Journal*, 18(4), 1269-1278.
27. Sahar,S H, Sura, K. I,Muhaned, A.M., & Mahasan, F. A. (2020). Synthesis and characterization of some metal complexes with new ligand ($C_{15}H_{10}N_4O_7SCl$) theoretical

treatment. *Systematic Reviews in pharmacy*, 11(12), 747-753.

28. Sahar, S. H., Sura, K. I., & Muhanned, A. M. (2018). Synthesis, characterization and theoretical study of some transition metal complexes with N-(4-(dimethyl amino benzylidene) benzo[d] thiozal-2-amine). *Materials Science and Engineering*, 454, 012124.
29. Seyed, J. P., Omid, A. B., Rauf, F., & Nasser, A. (2020). Removal of malachite green using carboxymethyl cellulose-gpolyacrylamide /montmorillonite nanocomposite hydrogel. *International Journalof Biological Macromolecules*, 159, 1122–1131.
30. Siva, S. S., Sai, K. A.,Venkataramana, B., &Vijaya, K.N. B. (2019). Development of poly (acrylamide-co-diallyldimethylammoniumchloride) nanogels and study of their ability as drug delivery devices. *Catylysts*, 9, 788.
31. Soubh, T., Bhawna, S., Ankit, V., Jyoti, C., Sigitas, T.V., & Vijay, K.T.(2018).Recent progress in sodium alginate based sustainable hydrogels for environmental applications. *Journal of cleaner production*, 198, 143-159.
32. Tabarek, M. Y., & Ahlam, M. A. (2023). Synthesis and Characterization of New Bis-Schiff Bases Linked to Various Imide Cycles. *Iraqi Journal of Science*, 64(3), 1062-1070.
33. Tian, Y., Du, C., Liu, B., Qiu, H. N., Zhang, X., Wu, Z. L., & Zheng, Q. (2021). Tough and fluorescent hydrogels composed of poly(hydroxyurethane) and poly (stearyl acrylate-co-acrylic acid) with hydrophobic associations and hydrogen bonds as the physical crosslinks. *Journal of Polymer Science*, 59(10), 904–911.
34. Uzma, Y.,Fazal, H.,Mehwish, K. , & Arshad, F.(2022). Synthesis of Starch-Grafted Poly Methyl methacrylate via Free Radical Polymerization Reaction and Its Application for the Uptake of Methylene Blue.*Molecules*, 27, 1-17.
35. Veena,S., Syed, S., Rama, G., Irfan, A., Rajib, B., & Nanthini,S. (2022). Comprehensive Review on Zeolite-Based Nanocomposites for Treatment of Effluents from Wastewater. *Nanomaterials*, 12, 1-29.
36. Veyan, T. S., Abbas, A. S. A. , Vian, Y. J., Mohammad, E. K., Adnan, D., Wail, A., & Young G. K. 2020. Phosphorus Schiff base ligand and its complexes: Experimental and theoretical investigations. *Applied Organometallic Chemistry*, 34, 1-16.
37. Wu,K. H., Wang, Y. R., & Hwu,W. H. 2003. FTIR and TGA studies of poly(4-vinylpyridine-co-divinylbenzene)–Cu (II)complex. *Polymer Degradation and Stability*, 79, 195–200.